Appendix. Longitudinal Analysis and Self-Registration (LASR) Algorithm

STEP 1: PERFORM SEGMENTATION ON IMAGES TO SEPARATE PIXELS IN BACKGROUND FROM SITTING CONTACT AREA

Although there are many segmentation algorithms for radiologic images, methods vary widely depending on the specific applications, imaging modality, and other factors. From the statistical point of views, all segmentation methods can be considered as classification techniques especially established for image analyses. Thresholding is a simple yet often effective means for obtaining segmentation in images where different structures have contrasting intensities or other quantifiable features [1-3]. In the current application, the pixel values of the pressure maps represent the applied pressure. It is reasonable to assume that an optimal threshold pressure will separate background noise from true contact area.

Segmentation minimizes both possible effects of the noise from background on the midline estimation (described below) and the boundary effect from smoothing described in Step 4 (**Appendix Figure 1**). Since intensity values at background pixels are much lower than those at sitting regions, the threshold segmentation method described below is optimal from the statistical point of view [4] and confirmed by **Appendix Table 1** below. Specifically, each data frame is partitioned into two distinct parts by classifying those less than a threshold T to the background and those greater than T to the sitting contact area. The value of T is estimated by first modeling the distribution of all pixels as a finite mixture of normal distributions of the form:

$$\alpha_1 f_1(x) + \alpha_2 f_2(x) + ... + \alpha_k f_k(x)$$

where f_i are normal densities, α_i's are nonnegative mixing parameters that sum to $\sum\alpha_i=1$, and k will be determined by a model selection procedure such as Akaike information criterion (AIC) or Bayesian information criterion (BIC) [5], and then computing the optimal threshold value T by a data-driven EM algorithm [6]that minimizes the expected misclassification rate (EMR) defined in [4]. The EMR is given by

$$EMR(T) = \left\{ \alpha_1 \int_T^{+\infty} f_1(z)dz + \int_{-\infty}^{T} [\alpha_2 f_2(s) + ... + \alpha_k f_k(s)]dz \right\}.$$

This EMR is the summation of the probability that a pixel value from the background (modeled by f_1) is misclassified to the sitting contact area plus the probability that a pixel value from a sitting contact area (modeled by $\alpha_2 f_2(x) + ... + \alpha_k f_k(x)$, proportionally) is misclassified into the background area, thus T is the value that minimizes EMR(T).All unknown parameters in the component densities f_i and mixing parameters α_1,…, α_k are estimated automatically by the EM algorithm. Note that in most cases a mixture of two or three normal distributions fits the density of pixels in a sitting region well (i.e. $k = 3$ or 4) .However, our estimate of T is relatively robust no matter whether we fit a 3- or 4- component normal mixture to the data. **Appendix Table 2** shows the true background and signal distributions as well as true k and T in the first three columns. The remaining columns in **Appendix Table 2** contain the average values and the standard deviations of the threshold value T estimated by our EM algorithm when k is specified either as 2, 3, or 4 based on the AIC for the same data sets from 100 simulation experiments, each with a sample size of 500. It is clear from this table that even when the estimate $\hat{k}$ is different from the true k, the estimated thresholds for correctly identified k (the boldfaced value), and incorrectly identified k are all very close to the true threshold. Hence our segmentation procedure is effective and robust against the variation in the estimate of k.

Appendix Table 1 further confirms the robustness of the threshold segmentation procedure for our problem by computing the exact threshold for signal distributions of various components. The first 5 rows show that the threshold changes minimally as long as the background distribution is the same and far away from the signal distribution. The number of components in the signal distribution has minimal effect on the threshold value. The last 5 rows show examples chosen to mimic the current study data. Other authors have started with one normal density for the signal region and then suggested "bias corrections" if there were more components in the signal region

[7]. Our method directly computes *k* by AIC or BIC and then computes the optimal *T* once for all, thus facilitating rapid data processing.

STEP 2: SPATIAL AND TEMPORAL REGISTRATION

Step 2.1 (Spatial Registration)

All images are spatially registered using our newly developed self-registration scheme [4, 8] as follows:

(a) Zero all pixel values in the background region.

(b) Estimate the "random landmarks": an end point and a midline (the human midline between two legs) by a regression analysis applied to "apparent middle points" equivalent to the mid-point of each column of an image.

(c) Transform the raw image into one that is centered at the midline and has the end point at the same place of the image. This step is done automatically for all images in a dataset (movie) so that all registered images are automatically standardized for future direct comparisons.

Step 2.2 (Temporal Registration)

If the two movies for comparison are both dynamic, the algorithm then also temporally registers the spatially registered movies. The temporal registration is based on a fast algorithm that aligns images at the same time point (i.e. a particular frame in one movie with another frame in another movie) by maximizing the correlation of intensities, i.e. pressure values, between images from two candidate movies so that the intensities are compared under the same conditions, i.e., they are compared pixel by pixel when both pixels are from the same location and are subject to the same dynamic stimulation. Specifically, we first throw away a few unstable images from both movies, let n be the remaining number of frames from each movie, and then align the first frame in movie one with jth frame of movie two, where j is the value that maximizes $(n-j)^{-1}\sum_i cor(A_i, B_{i+j})$, and A_i, B_i indicate the intensity values of the i th image frame from two movies. Thus the left

side stimulated image in one movie is compared with the left-side stimulated image in another movie. See movies at stat.case.edu/lasr/.

STEP 3: CREATE DIFFERENCE MAPS/MOVIES

Difference images and movies are created by taking differences pixel-by-pixel (and frame-by-frame) between two movies that are potentially clinically interesting. In the current study all difference images and movies were created between the first dataset collected at baseline assessment and the last dataset of the final assessment in the available time series.

STEP 4: COMPUTE FILTERED MAPS/MOVIES

A nonparametric filtering procedure is important because we do not have a-priori knowledge of the shape of the differences between pairs of movies to postulate a parametric model. A local-polynomial smoothing technique is used that keeps the local distribution structure while filtering out noise. We first padded an image at a small neighborhood of a sitting region (segmented out by Step 1) with the pixel value at the edge of the sitting region and then used smoothing to filter the image on this extended region (the sitting region plus the neighborhood) and finally “cut back" the image to the sitting region to avoid the boundary effect which can occur with any nonparametric smoothing procedure. This padding idea is similar in spirit to that used in Charnigo et al [9] for their semi-local denoising paradigm [9].

Step 5: CREATE T IMAGE/MAPS AND MOVIES

T images are obtained by computing a test statistic at each pixel in the spirit of a two-sample paired t-test but differs from the t-test in the following way; our test statistic at each pixel x is $T_x = D_x/S_x$, where D_x is the pixel value of a filtered difference image, i.e. a weighted average of the difference values in a neighborhood of x from a difference image obtained in Step 4 (versus a simple average of an independent and identically distributed sample drawn at the same location x, in a two-sample *t*-test scenario), and S_x is an appropriately estimated standard deviation of D_x. We then computed the individual significance, or P value, of each pixel difference.

Step 6: COMPUTE AND CREATE FALSE DISCOVERY RATE-CONTROLLED *P* MAPS/MOVIES

Each of the individual P values from Step 5 allows us to decide if two images are significantly different at that pixel. However, there are many pixels in an image that are examined simultaneously, called multiple comparisons in statistics. We must therefore use an effective procedure to control a global error rate for this multiple testing problem, as mentioned above. The false discovery rate (FDR) is the expected value of "the percentage of false discoveries among all claimed discoveries" [10]. Here the discoveries are all the pixels at which there are significant differences/changes. The threshold for controlling such a FDR at 0.05 is often smaller than a simple 0.05 cut-off value used for a single test (here a single pixel) unless the number of pixels is one. A basic 0.05 FDR-controlled threshold is that defined by Benjamini and Hochberg [10]. **Appendix Figure 2** illustrates how a level-α FDR-controlled threshold is computed: (1) sort all individual *p*-values computed at each pixel based on an approximate *t*-distribution, in an ascending order, so they are now $p_{(1)} \le p_{(2)} \le ... \le p_{(m)}$, where *m* is the number of pixels; (2) plot them against *1:m*; (3) find the largest index value i in *1:m* at which these sorted p-values does not cross the straight line $y = (i/m)\,\alpha$, call this index value *k*; and (4) the level-α FDR-controlled threshold is then $p_{(k)}$, which can be written mathematically as

$$p_{(k)} = \max\{p_{(i)} : 1 \le i \le m, p_{(i)} \le \frac{i}{m}\alpha\}.$$

Zhang's work [11] contains an improvement to the above threshold definition. Then all the pixels with individual p-values less than this $p_{(k)}$ (often much smaller than α) are deemed active or significant. In building our FDR-controlled *P* maps or movies if a *P* value *p* at a pixel x is less than the critical value $p_{(k)}$, we change the pixel value to $1 - p$. If p is greater than the FDR cut-off value, the pixel value is set to zero. The resulting FDR-controlled P maps or movies show areas with significantly decreased interface pressures, implying improved tissue health.

Appendix Figure 1.

Effects of segmentation on boundary properties. After segmentation image shows location of midline, defined as the midline between legs, and endpoint, defined as intersection of midline and posterior margin of region of interest.

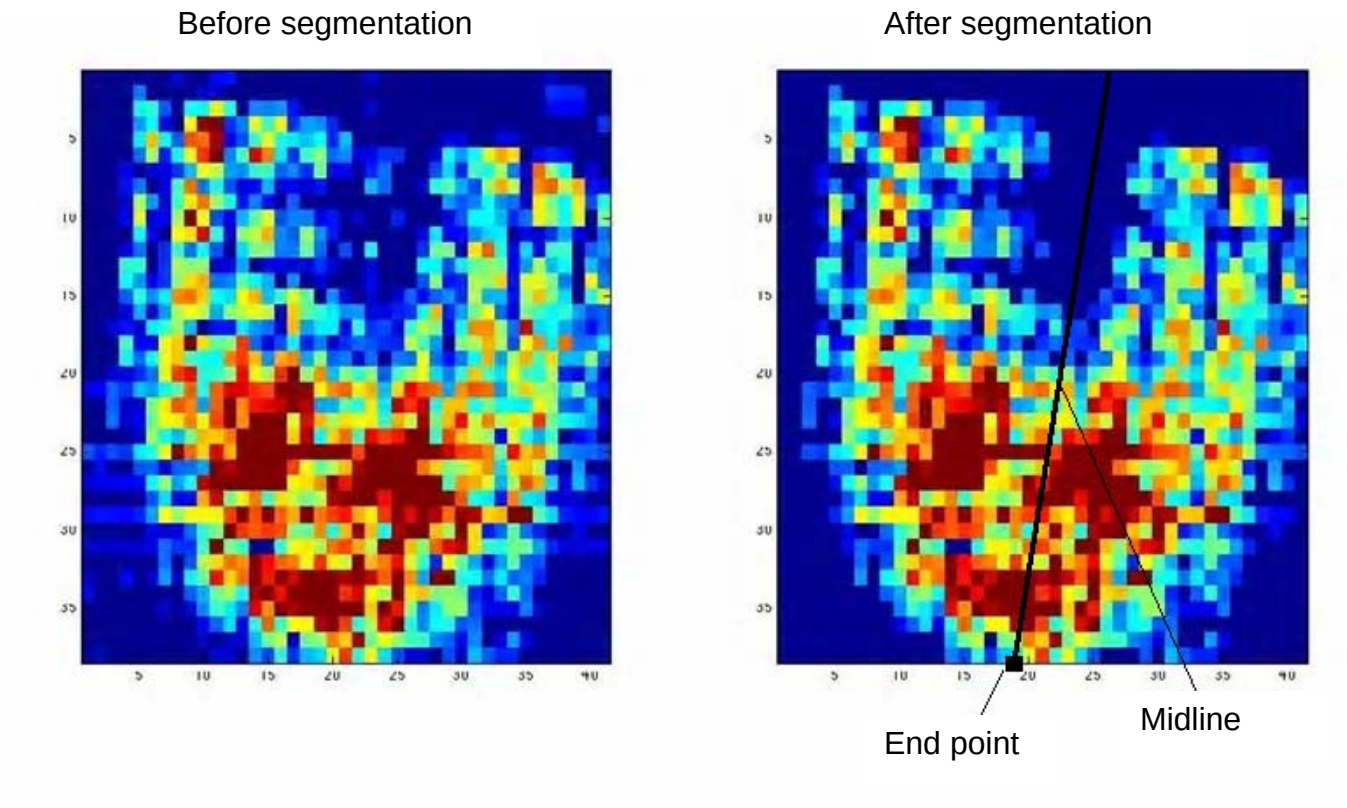

Appendix Table 1.

Robustness of Methods. N(a,b) denotes the normal distribution with mean *a* and variance *b*.

Background distribution	Signal distribution	True threshold	True Value k
0.2*N(0,1)	0.8*N(5,1)	2.22	2
0.2*N(0,1)	0.4*N(5,1)+0.4*N(8,1)	2.36	3
0.2*N(0,1)	0.4*N(5,1)+0.4*N(10,1)	2.36	3
0.2*N(0,1)	0.3*N(5,1)+0.3*N(7,0.5)+0.2*N(11,0.5)	2.41	4
0.2*N(0,1)	0.3*N(5,1)+0.2*N(8,0.5)+0.3*N(10,0.5)	2.41	4
0.4*N(0,2)	0.6*N(10,1)	6.45	2
0.4*N(0,2)	0.3*N(10,1)+0.3*N(12,1)	6.58	3
0.4*N(0,2)	0.4*N(10,1)+0.2*N(12,1)	6.53	3
0.4*N(0,2)	0.3*N(10,1)+0.2*N(12,1)+0.1*(14,1)	6.58	4
0.4*N(0,2)	0.3*N(10,1)+0.2*N(11,1)+0.1*(15,2)	6.58	4

Appendix Table 2.

Simulation for robustness of expectation maximization (EM) segmentation method. N(a,b) denotes the normal distribution with mean *a* and variance *b*.

Background distribution	Signal distribution	True threshold	True k	EM estimate for threshold (Mean±SD)		
				$\hat{k}=3$	$\hat{k}=2$	$\hat{k}=4$
0.3*N(0,1)	0.3*N(5,1)+0.4*N(10,0.5)	2.50	3	2.51±0.08	2.49±0.07	2.55±0.07
0.5*N(0,0.5)	0.3*N(5,1)+0.2*N(10,0.5)	1.78	3	1.79±0.06	1.81±0.05	1.83±0.05
0.5*N(0,1)	0.5*N(10,1)	5.00	2	5.03±0.07	4.98±0.07	5.05±0.06
0.5*N(0,2)	0.5*N(10,1)	6.53	2	6.55±0.06	6.54±0.08	6.55±0.06
0.3*N(0,1)	0.3*N(10,1)+0.4*N(12,1)+0.2*(14,2)	4.80	4	4.82±0.05	4.79±0.07	4.84±0.06
0.5*N(0,2)	0.2*N(10,1)+0.2*N(12,1)+0.1*(14,2)	6.69	4	6.71±0.06	6.66±0.07	6.70±0.07

SD= standard deviation.

Appendix Figure 2.

Principle of false discovery rate.

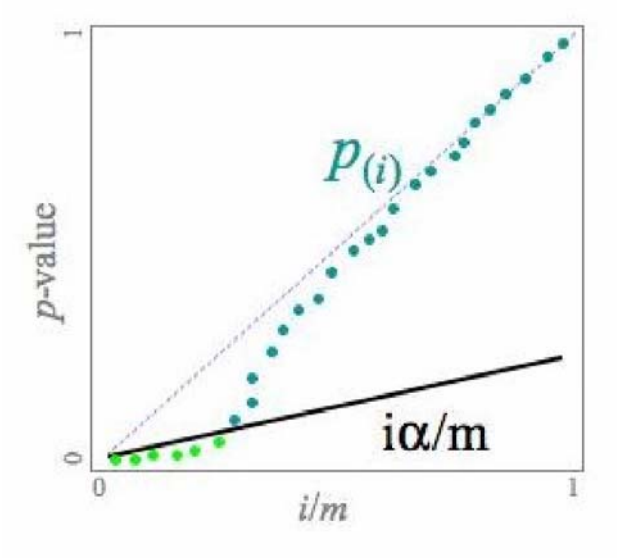

REFERENCES

1. Kittler J, Illingworth J. Minimum error thresholding. Pattern Recognit. 1986;19(1):41–47.

2. Mardia KV, Hainsworth TJ. A spatial thresholding method for image segmentation. IEEE Trans Pattern Anal Mach Intell. 1998;10(6):919–27.

3. Tobias OJ, Seara R. Image segmentation by histogram thresholding using fuzzy sets. IEEE Trans Image Process. 2002;11(12):1457–65. [PMID: 18249714]

4. Wang X, Sun J, Bogie K. Spatial-temporal data mining procedure: LASR. In: Sun J, DasGupta A, Melfi V, Page C, editors. Recent developments in nonparametric inference and probability: Festschrift for Michael Woodroofe. Beachwood (OH): Institute of Mathematical Statistics; 2006. p. 213–31.

5. Aissaoui R, Kauffmann C, Dansereau J, de Guise JA. Analysis of pressure distribution at the body-seat interface in able-bodied and paraplegic subjects using a deformable active contour algorithm. Med Eng Phys. 2001;23(6):359–67. [PMID: 11551812] Erratum in: Med Eng Phys. 2001;23(10):745.

6. Dempster AP, Laird NM, Rubin DB. Maximum likelihood from incomplete data via the EM algorithm. J Royal Stat Soc Ser B Methodol. 1977;39(1):1–38.

7. Maintz JB, Viergever MA. A survey of medical image registration. Med Image Anal. 1998;2(1):1–36. [PMID: 10638851]

8. Wang X. New procedures for data mining and measurement error models with medical imaging applications [dissertation]. Cleveland (OH): Department of Statistics, Case Western Reserve University; 2005.

9. Charnigo R, Sun J, Muzic R Jr. A semi-local paradigm for wavelet denoising. IEEE Trans Image Process. 2006;15(3):666–77. [PMID: 16519353]

10. Benjamini Y, Hochberg Y. Controlling the false discovery rate: A practical and powerful approach to multiple testing. J Royal Stat Soc Ser B Methodol. 1995;57(1):289–300.

11. Zhang Z. Multiple hypothesis testing for finite and infinite number of hypotheses [dissertation]. Cleveland (OH): Department of Statistics, Case Western Reserve University; 2005.